

Hypoxia is important in F-18 FDG accumulation in thecoma-fibroma tumors on F-18 FDG PET/CT scans

HIROKO SEINO^{1,2}, SHUICHI ONO¹, HIROYUKI MIURA¹, SATOKO MOROHASHI², YUNYAN WU², FUMIYASU TSUSHIMA¹, YOSHIHIRO TAKAI¹ and HIROSHI KIJIMA²

Departments of ¹Radiology and Radiation Oncology and ²Pathology and Bioscience, Hirosaki University Graduate School of Medicine, Hirosaki, Aomori 036-8562, Japan

Received November 8, 2014; Accepted August 4, 2015

DOI: 10.3892/mmr.2016.5016

Abstract. Several studies have noted benign thecoma-fibroma tumors with positive F-18 fluorodeoxyglucose (FDG) accumulation mimicking malignant ovarian tumors following F-18 FDG positron emission tomography (PET). The present study analyzed four cases with false-positive F-18 FDG PET/computed tomography (CT) diagnoses of thecoma-fibroma tumors as malignant tumors due to F-18 FDG accumulation, compared with eight cases of FDG-positive ovarian cancers and two cases of FDG-negative fibromas. Hypoxia inducible factor (HIF)-1 α expression was examined in the six thecoma-fibroma tumors using reverse transcription-polymerase chain reaction (RT-PCR). The four F-18 FDG-positive cases exhibited higher cellularity, maximum standard uptake and signal intensity on T2-weighted imaging, and gadolinium (Gd) enhancement using magnetic resonance imaging than the two FDG-negative fibroma cases. In the F-18 FDG-positive thecoma-fibroma group, Ki-67 expression was low and LAT1 expression was not identified, ruling out the diagnosis and potential for malignancy. However, considerable glucose transporter 1, HIF-1 α , and vascular endothelial growth factor expression was observed. HIF-1 α expression was elevated in all four false-positive cases by RT-PCR. From these results, it was hypothesized that hypoxia due to elevated cellularity may stimulate HIF-1 α expression and be associated with F-18 FDG accumulation in F-18-positive thecoma-fibroma tumors.

Introduction

The thecoma-fibroma group, a subgroup of ovarian sex cord-stromal tumors, encompasses a spectrum of neoplasms

ranging from those entirely composed of lipid-containing cells resembling theca interna cells to those containing predominantly spindle-shaped cells with variable intercellular collagen. Although these tumors are benign and relatively rare, accounting for 3-4% of all ovarian tumors (1), they represent the most common type of solid primary ovarian tumors. Fibromas are purely composed of mature fibroblastic cells producing abundant collagen, whereas thecomas contain numerous cells resembling theca and/or lutein cells and a number of fibroblasts. However, it is occasionally difficult to differentiate between fibroma and thecoma, thus justifying the use of the term thecoma-fibroma tumor. There have been several studies of thecoma-fibroma tumors with positive F-18 fluorodeoxyglucose (FDG) accumulation mimicking malignant ovarian tumors (2,3). To the best of our knowledge, none of those studies described the detailed causes of F-18 FDG accumulation. Therefore, it was hypothesized that these false-positive findings may be associated with tumor vascularity and/or proliferation as a number of thecoma-fibroma tumors appear as hypovascular tumors with delayed weak enhancement in dynamic contrast magnetic resonance imaging (MRI) studies (4). Furthermore, cellular fibroma is known as to possess an uncertain malignant potential (5); in other words, imbalances between the cell density and blood supply, malignant formation, and/or other conditions may induce F-18 FDG accumulation by altering the glucose metabolism. In this study, the cause of F-18 FDG accumulation in thecoma-fibroma tumors was investigated by addressing passive tumor ischemia/hypoxia and malignant potential in these tumors and comparing these tumors with F-18 FDG-negative fibromas and malignant ovarian tumors.

Materials and methods

Patients. The Research Ethics Committee of the Hirosaki University Graduate School of Medicine/University Hospital (Hirosaki, Japan) approved this retrospective study and waived the requirement for individual patient consent. From 2008 to 2013, 78 female patients underwent preoperative F-18 FDG positron emission tomography (PET)/computed tomography (CT) scans for various ovarian tumors at the Hirosaki University Hospital. Of these 78 cases, 46 were pathologically proven to be malignant and 32 were benign.

Correspondence to: Dr Hiroshi Kijima, Department of Pathology and Bioscience, Hirosaki University Graduate School of Medicine, 5 Zaifu-cho, Hirosaki, Aomori 036-8562, Japan
E-mail: hkijima@hirosaki-u.ac.jp

Key words: F-18 fluorodeoxyglucose positron emission tomography/computed tomography, thecoma-fibroma group, false-positive, F-18 fluorodeoxyglucose uptake

The sensitivity and specificity of the PET findings were 93.5 and 83.9%, respectively, for distinguishing malignant ovarian tumors from benign ovarian lesions using a maximum standard uptake value (SUV_{max}) cutoff of 2.5. Of the 32 benign cases, six were analyzed as they showed positive FDG accumulation mimicking malignant ovarian tumors (four cases of thecoma-fibroma tumors and two cases of xanthogranulomatous inflammation) with positive F-18 FDG accumulation. The details of the four FDG-positive thecoma-fibroma tumor cases are shown in Table I. One case (fibroma, SUV_{max}=4.0) exhibited mild cystic degeneration, whereas the other three cases (cellular fibroma, SUV_{max}=5.2; thecoma-fibroma tumor, SUV_{max}=2.7; and fibroma, SUV_{max}=4.1) exhibited severe cystic degeneration. For comparison, two fibroma cases with negative F-18 FDG accumulation (Table II) were selected and eight malignant ovarian tumor cases (SUV_{max} <5.5) without metastasis or invasion and with undetermined malignant statuses according to SUV_{max} alone due to the relatively low values (Table III).

F-18 FDG PET/CT and image analysis. In preparation for PET/CT, all patients fasted for at least 4 h and water intake was encouraged. F-18 FDG (FDG scan injectable, 185 MBq on the assay date; Nihon Medi-Physics, Tokyo, Japan) was delivered via intravenous injection ~60 min prior to the initiation of scanning. During the 60-min uptake period, the patients were advised to drink a sufficient amount of water and to remain calm. A PET/CT system (Discovery ST Elite 16; GE Healthcare, Milwaukee, WI, USA) was used to acquire all data in 7-8 bed positions with an acquisition time of 2.5-3.0 min per bed position. CT was performed first (30-80 mA, 120 kV, 3.75-3.27-mm slice thickness). The CT data were used for attenuation correction of PET data as well as for co-registration with the attenuation-corrected PET images. The PET data of the same body regions were acquired immediately following CT imaging. The PET, CT, and fused PET/CT images were available for review and were displayed in the axial, coronal, and sagittal planes on a viewer system (Discovery ST Elite 16; GE Healthcare). SUV_{max} (g/ml) was evaluated in all histopathologically proven lesions, as described previously (4).

MRI and image analysis. MRI examinations were performed on a 3.0-T unit (Signa HDxt, GE Healthcare) or a 1.5-T unit (Magnetom Vision; Siemens AG, Erlangen, Germany or Signa HDxt).

The MRI characteristics of each thecoma-fibroma tumor were recorded separately and included the following items: Lesion components (solid, cystic, solid with cystic components, or cystic with solid components), signal intensity on T2-weighted imaging (WI) (hypointensity, isointensity, or hyperintensity), and gadopentetate dimeglumine (Gd-DTPA) enhancement (mild, moderate or severe). The signal intensity of each lesion on T2WI was quantitatively compared with that of the uterine myometrium and iliopsoas muscle. On T2WI, the hypointensity and hyperintensity of the pelvic wall muscle and fat signals were similar. After the intravenous injection of contrast medium, the degree of lesion enhancement was graded as follows: Mild enhancement (less than the myometrium), moderate enhancement (similar to the myometrium), or severe enhancement (greater than the myometrium).

Histological analysis. For the histological examination, specimens of the six thecoma-fibroma tumors and eight malignant tumors were routinely fixed in formalin, embedded in paraffin, sectioned into thin slices, and stained with hematoxylin-eosin. Thin (4- μ m) sections were mounted on silane-coated glass slides (Matsunami Glass Industry, Ltd., Osaka, Japan). A standard automated immunostainer (Benchmark XT; Ventana Medical Systems, Tucson, AZ, USA) was used to perform an immunohistochemical examination of the deparaffinized sections. The following antibodies were used: Polyclonal rabbit anti-human glucose transporter 1 (GLUT1; 1:200 dilution; cat. no. ab15309; Abcam, Cambridge, UK), monoclonal mouse anti-human L-type amino acid transporter 1 (LAT-1; 1:50; clone LAT-1; cat. no. M7279; Dako, Glostrup, Denmark), monoclonal mouse anti-human hypoxia-inducible factor 1 α (HIF-1 α ; 1:100; clone HIFa67; cat. no. MAB5382; Millipore, Billerica, MA, USA), polyclonal rabbit anti-human vascular endothelial growth factor (VEGF; 1:100; cat. no. A-20; Santa Cruz Biotechnology, Inc., Santa Cruz, CA, USA), and monoclonal mouse anti-human Ki-67 (1:100; clone MIB-1; cat. no. M7248; Dako). The GLUT1, LAT1, HIF-1 α , and VEGF immunohistochemical reactions were semiquantitatively scored as follows: 0, negative; 1, weak; 2, intermediate; and 3, strong. Images of the immunohistochemical analyses were captured using a BX50 microscope and DP70 digital camera (Olympus Corporation, Tokyo, Japan).

Reverse transcription-polymerase chain reaction (RT-PCR). For RNA preparation from the formalin-fixed, paraffin-embedded (FFPE) fibroma-thecoma tumor tissue sections, the RNeasy FFPE kit (Qiagen GmbH, Hilden, Germany) was used according to the manufacturer's instructions. RT-PCR of an aliquot of first-strand cDNA as the template was performed under standard conditions with Taq DNA polymerase (Qiagen GmbH). The primers were as follows: HIF-1 α -F: 5'-AGCCCTAGATGGCTTTGTGA-3', HIF-1 α -R: 5'-TATCGAGGCTGTGTCGACTG-3', GAPDH-F: 5'-CCACCCATGGCAAATTCCATGGCA-3', and GAPDH-R: 5'-AGACCACCTGGTGCTCAGTGTAGC-3'. The amplified products of the HIF-1 α and GAPDH primers were 466 and 696 base pairs in length, respectively. HIF-1 α and GAPDH cDNA were amplified for up to 25 cycles (94°C for 40 sec, 59°C for 40 sec and 72°C for 40 sec) using a C1000 Touch Thermal Cycler (Bio-Rad Laboratories, Inc., Hercules, CA, USA). The PCR products were separated on 1.5% (w/v) agarose gels (UltraPure Agarose; Invitrogen; Thermo Fisher Scientific, Inc., Waltham, MA, USA).

Results

Imaging and pathological findings of thecoma-fibroma tumors. The four false-positive cases exhibited higher cellularity, SUV_{max}, signal intensity on T2WI, and Gd-DTPA enhancement on MRI than the two negative fibroma cases (Table IV). Increases in FDG uptake and Gd-DTPA enhancement in the tumor tended to occur near the areas of severe cystic degeneration. Histologically, the four false-positive tumors comprised an area of high cellularity and an edematous or degenerated hypocellular area. In the cellular area, spindle-shaped tumor cells were randomly distributed or arranged in a fascicular manner. By contrast, the edematous or

Table I. Benign F-18 fluorodeoxyglucose-positive cases (n=4).

Patient	Age (years)	Pathology	Tumor form	Size (cm)	Ascites	Hyperestrogenism	CA125
1	67	Fibroma	SWCC	15	Little	None	186
2	56	Cellular fibroma	CWSC	5	Massive	None	16
3	69	Thecoma-fibroma tumors	CWSC	20	Little	None	144
4	67	Fibroma	CWSC	21	Massive	None	813

SWCC, solid with cystic components; CWSC, cystic with solid components.

Table II. Benign F-18 fluorodeoxyglucose-negative cases (n=2).

Patient	Age (years)	Pathology	Tumor form	Size (cm)	Ascites	Hyperestrogenism	CA125
1	31	Fibroma	Solid	13	Little	None	24
2	51	Fibroma	Solid	4	None	None	10

Table III. Malignant cases (n=8).

Patient	Age (years)	Pathology	Tumor form	Size (cm)	Ascites	SUVmax	CA125
1	59	Serous adenocarcinoma	CWSC	15	None	4.8	11
2	46	Serous adenocarcinoma	CWSC	15	Little	2.4	101
3	29	Serous adenocarcinoma	CWSC	13	Little	5.2	10
4	36	Serous adenocarcinoma	Cystic	17	Little	<1.0	11
5	37	Serous adenocarcinoma	CWSC	3	None	3.9	30
6	61	Clear cell adenocarcinoma	SWCC	9	None	4.7	40
7	59	Clear cell adenocarcinoma	CWSC	20	Little	4.5	526
8	34	Mucinous adenocarcinoma	CWSC	16	None	3.5	89

SUV, standard uptake value; SWCC, solid with cystic components; CWSC, cystic with solid components.

Table IV. Imaging and pathological findings of thecoma-fibroma tumors (n=6).

PET	Pathological findings	Size (cm)	SUVmax	T2WI	Gd-DTPA enhancement
Negative	F>HC	13	2.2	Low intensity	Mild
Negative	F>HC	4	2.4	Low intensity	Mild
Positive	HC>F	15	4.0	High intensity	Moderate
Positive	HC>F	5	5.2	High intensity	Severe
Positive	HC>F	20	2.7	High intensity	Severe
Positive	HC>F	21	4.1	High intensity	Severe

PET, positron emission tomography; SUV, standard uptake value; WI, weighted imaging; Gd, gadopentetate dimeglumine; F, fibrous component; HC, high-cellular component.

degenerated area contained scattered spindle or stellate cells without atypia (Fig. 1).

Immunohistochemical findings and RT-PCR analysis. SUVmax (Fig. 2A) and levels of HIF-1 α , VEGF, LAT1, Ki-67,

and GLUT1 expression in the malignant ovarian tumors tended to be higher than those in the false-positive and negative thecoma-fibroma tumors. The false-positive thecoma-fibroma group exhibited low levels of Ki-67 expression and no LAT1 expression. However, these lesions expressed considerable

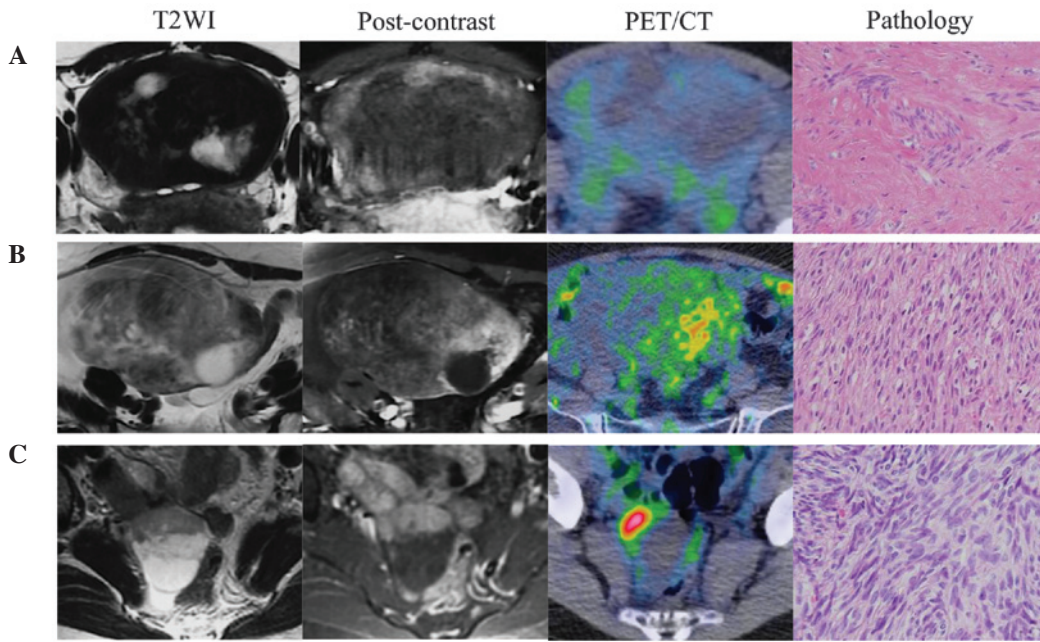


Figure 1. Imaging and pathological findings of thecoma-fibroma tumors. (A) F-18 FDG-negative fibroma on PET. The low signal intensity, comparable with that of muscle tissue, was typical of fibroma. The tumor, comprising small spindle cells that produce large amounts of collagen, contained scattered areas of high signal intensity representing edema degeneration on T2-weighted MRI. Weak FDG uptake was observed. A diagnosis of benign disease was easily made from these imaging findings. (B) F-18 FDG-positive fibroma. The tumor exhibited higher signal intensity relative to that of the muscle tissue on T2-weighted MRI. A solid component near the area of cystic degeneration exhibited stronger enhancement and increased FDG uptake. Pathological analysis of the tumor revealed elevated cellular proliferation. (C) F-18 FDG-positive cellular fibroma. The tumor appeared as a cystic neoplasm with a solid component; the latter exhibited strong enhancement on T1-weighted MRI and elevated FDG uptake. Pathological analysis of the tumor revealed elevated cellular proliferation. Magnification, x40. FDG, fluorodeoxyglucose; PET, positron emission tomography; MRI, magnetic resonance imaging.

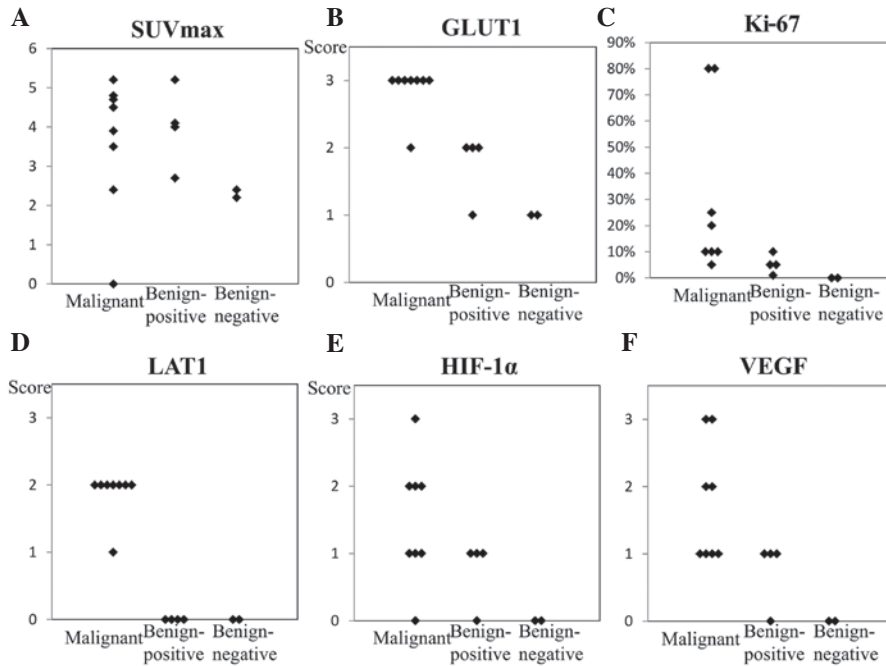


Figure 2. SUVmax (A) and immunohistochemical analysis findings of (B) GLUT1, (C) Ki-67, (D) LAT1, (E) HIF-1 α and (F) VEGF expression in the imaged lesions. In the malignant ovarian tumors, HIF-1 α , VEGF, LAT1, Ki-67, and GLUT1 expression tended to be relatively higher than that in the thecoma-fibroma group. In the F-18 FDG-positive thecoma-fibroma group, Ki-67 expression was low and LAT1 expression was absent, thereby excluding the possibility of malignancy in these lesions. However, considerable GLUT1, HIF-1 α , and VEGF expression were observed. In the two cases of F-18 FDG-negative fibroma, HIF-1 α , VEGF, LAT1, Ki-67 and GLUT1 expression levels were low or inconclusive. SUV, standard uptake value; GLUT1, glucose transporter 1; LAT1, L-type amino acid transporter 1; HIF-1 α , hypoxia-inducible factor 1 α ; FDG, fluorodeoxyglucose.

quantities of GLUT1, HIF-1 α and VEGF. In the two cases of FDG-negative fibromas, levels of HIF-1 α , VEGF, LAT1,

Ki-67, and GLUT1 expression were low or inconclusive. In the malignant ovarian tumors, the levels of HIF-1 α , VEGF,

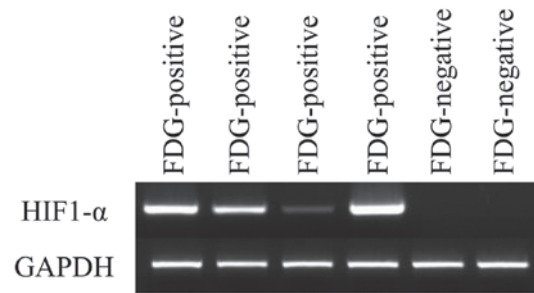


Figure 3. Reverse transcription-quantitative polymerase chain reaction to evaluate HIF-1 α expression in cases of thecoma-fibroma. The expression levels were increased in all four F-18 FDG positive cases but not in the two negative cases. HIF, hypoxia inducible factor; FDG, fluorodeoxyglucose.

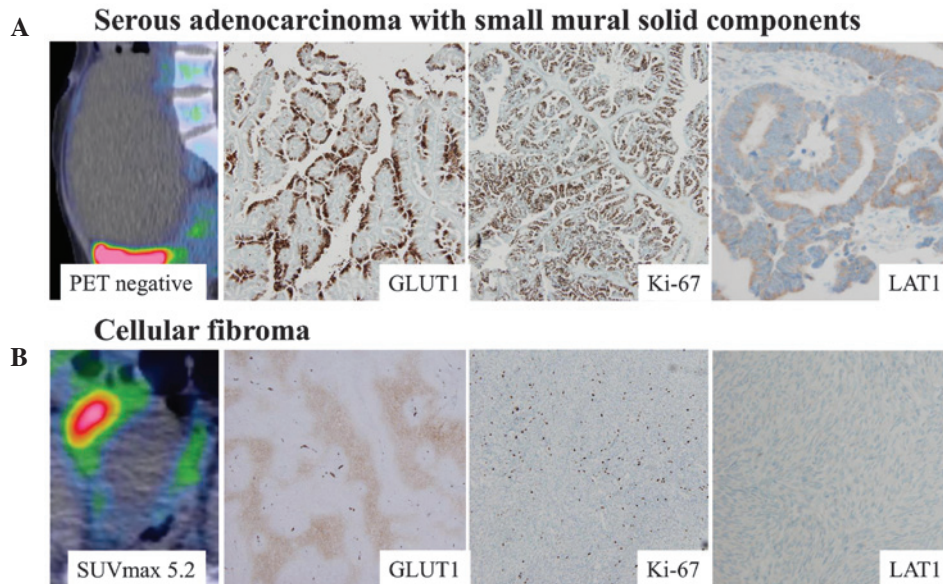


Figure 4. Imaging and immunohistochemical findings of adenocarcinoma and fibroma. (A) A serous adenocarcinoma diagnosed as a benign lesion from preoperative PET and MRI findings. Clinicopathologically, GLUT1, Ki-67 and LAT1 expression levels were elevated. (B) An F-18 FDG-positive cellular fibroma exhibited negative Ki-67 and LAT1 expression, despite positive GLUT1 expression. Magnification, x40. PET, positron emission tomography; MRI, magnetic resonance imaging; GLUT1, glucose transporter 1; LAT1, L-type amino acid transporter 1; FDG, fluorodeoxyglucose.

LAT1, Ki-67 and GLUT1 expression varied from high to low (Fig. 2B-F).

HIF-1 α expression was elevated in all F-18 FDG-positive thecoma-fibroma tumors (Fig. 3). By contrast, HIF-1 α expression was not observed in any FDG-negative fibromas. Thecoma-fibroma tumors with high cellular components exhibited positive F-18 FDG accumulation and immunohistochemical GLUT1 expression, whereas negative Ki-67 and LAT1 expression was observed (Fig. 4).

Discussion

In FDG PET, accumulation is determined by the delivery of FDG to the tissues, as well as the expression and activity levels of glucose transporter (GLUT) and hexokinase (HK). HIF-1 activates the transcription of GLUT1 and GLUT3, as well as HK, the first enzyme in the glycolytic pathway (6). HIF-1, a heterodimer composed of two subunits termed HIF-1 α and HIF-1 β , was identified following the identification of a hypoxia response element (HRE) (7,8). HIF-1 α expression remains low under physiological oxygen pressure in normal tissues and increases in response to systemic

hypoxia, whereas HIF-1 β is constitutively expressed regardless of the oxygen availability. Under hypoxic conditions, the HIF-1 α protein is stabilized and initiates a multistep activation pathway that includes nuclear translocation, dimerization with HIF-1 β , transcriptional coactivator recruitment, and subsequent binding to HREs of target genes (9). HIF-1 α , which induces the expression of erythropoietin (EPO) (10) and other oxygen-regulated genes, such as VEGF (11,12) and GLUT1 (13), and several glycolytic enzymes (14-16), has been shown to be important in various types of cancer through processes, such as tumor proliferation, tumor invasion, inflammation and ischemia (17-19). The results of the present study demonstrated that HIF-1 α expression was increased in all four F-18 FDG-positive thecoma-fibroma tumors. Accordingly, it was suggested that the upregulated HIF-1 α expression in these F-18 cases was correlated with increased GLUT1 and VEGF expression, thereby leading to F-18 FDG accumulation and stronger Gd-DTPA enhancement in MRI compared with the two negative fibroma cases.

In addition, elevated cellularity was also observed in all four F-18 FDG-positive thecoma-fibroma tumors. The majority of thecoma-fibroma tumor cases involve hypovascular tumors, as

determined by delayed weak enhancement in dynamic contrast MRI studies. Therefore, it was hypothesized that this increased cellularity induces ischemic changes and hypoxia in the tumor, thereby upregulating HIF-1 α expression. The hypoxia consequent to this increased cellularity stimulated HIF-1 α expression, leading to subsequent responses, such as GLUT1 and VEGF expression and resulting in F-18 FDG accumulation and strong enhancement. Notably, within the same tumor, the areas of F-18 FDG accumulation and stronger Gd-DTPA enhancement were observed near areas of severe cystic or hyaline degeneration, where hypoxia would be expected. A recent study revealed novel O₂-independent regulatory mechanisms of HIF transactivation such as mammalian target of rapamycin (mTOR) activation or altered mitochondrial metabolism, NAD⁺ levels, and nitric oxide levels (20); however, no studies have discussed the correlation between glucose metabolism and O₂-independent HIF regulation in thecoma-fibroma tumors.

Although thecoma-fibroma tumors are rarely malignant, certain tumor types included in the thecoma-fibroma group, such as cellular fibroma, have been recognized as having uncertain malignant potential (21). Similarly, malignant transformation induces hypoxia and consequently upregulates HIF-1 α expression. However, LAT-1 and Ki-67 labeling index immunostaining did not suggest malignant potential in the four false-positive cases. LAT-1 is specifically expressed in malignant tumors (22), and the Ki-67 labeling index is a classic cellular proliferation marker. Thus, if malignant potential had been detected in the false-positive cases, levels of LAT-1 or Ki-67 expression should have been increased. Lee *et al* (23) noted that the luteinized theca-like cells, which may continuously secrete vascular permeability factors and VEGF, thereby inducing angiogenesis, led to hypervascularity in ovarian sex cord-stromal tumors. However, this theory does not explain all four of the false-positive cases as only one thecoma-fibroma tumor case contained theca cells. Furthermore, clear differences in VEGF expression between the theca and fibroma cells were not observed in the thecoma-fibroma tumors.

One limitation of this study was the relatively small numbers of cases; this occurred because the incidence of thecoma-fibroma lesions is low (1), and PET/CT evaluations are not performed during clinical diagnosis of all thecoma-fibroma lesions. Thus, further studies are required to validate the present results. However, to the best of our knowledge, the present study demonstrated the first evidence of upregulated HIF-1 α expression in a false-positive thecoma-fibroma tumor on FDG/PET from a clinicopathological viewpoint.

Benign thecoma-fibroma tumors occasionally exhibit positive F-18 FDG accumulation mimicking malignant ovarian tumors. Elevated cellularity of the thecoma-fibroma tumor is thought to induce intratumoral hypoxia, leading to an upregulation of HIF-1 α expression and a subsequent increase in glucose metabolism. Intratumoral hypoxia may result in F-18 FDG accumulation. Benign thecoma-fibroma tumors with positive F-18 FDG accumulation should therefore be listed as one of the potential differential diagnoses of ovarian carcinoma.

Acknowledgements

This study was supported by Grants-in-Aid for Science from the Ministry of Education, Culture, Sports, Science,

and Technology of Japan; a grant for Hirosaki University Institutional Research; and the Fund for the Promotion of International Scientific Research.

References

1. Salemis NS, Panagiotopoulos N, Papamichail V, Kiriakopoulos K and Niakas E: Bilateral ovarian fibrothecoma. An uncommon cause of a large pelvic mass. *Int J Surg Case Rep* 2: 29-31, 2011.
2. Fenichel S, Kotzerke J, Stöhr I, Grab D, Nüssle K, Rieber A, Kreienberg R, Brambs HJ and Reske SN: Preoperative assessment of asymptomatic adnexal tumors by positron emission tomography and F 18 fluorodeoxyglucose. *Nuklearmedizin* 38: 101-107, 1999 (In German).
3. Fenichel S, Grab D, Nuessle K, Kotzerke J, Rieber A, Kreienberg R, Brambs HJ and Reske SN: Asymptomatic adnexal masses: Correlation of FDG PET and histopathologic findings. *Radiology* 223: 780-788, 2002.
4. Schwartz RK, Levine D, Hatabu H and Edelman RR: Ovarian fibroma: Findings by contrast-enhanced MRI. *Abdom Imaging* 22: 535-537, 1997.
5. Adad SJ, Laterza VL, Dos Santos CD, Ladeia AA, Saldanha JC, da Silva CS, E Souza LR and Murta EF: Cellular fibroma of the ovary with multiloculated macroscopic characteristics: Case report. *Case Rep Med* 2012: 283948, 2012.
6. Iyer NV, Kotch LE, Agani F, Leung SW, Laughner E, Wenger RH, Gassmann M, Gearhart JD, Lawler AM, Yu AY and Semenza GL: Cellular and developmental control of O₂ homeostasis by hypoxia-inducible factor 1 alpha. *Genes Dev* 12: 149-162, 1998.
7. Wang GL and Semenza GL: Purification and characterization of hypoxia-inducible factor 1. *J Biol Chem* 270: 1230-1237, 1995.
8. Wang GL, Jiang BH, Rue EA and Semenza GL: Hypoxia-inducible factor 1 is a basic-helix-loop-helix-PAS heterodimer regulated by cellular O₂ tension. *Proc Natl Acad Sci USA* 92: 5510-5514, 1995.
9. Wenger RH and Gassmann M: Oxygen(es) and the hypoxia-inducible factor-1. *Biol Chem* 378: 609-616, 1997.
10. Semenza GL and Wang GL: A nuclear factor induced by hypoxia via de novo protein synthesis binds to the human erythropoietin gene enhancer at a site required for transcriptional activation. *Mol Cell Biol* 12: 5447-5454, 1992.
11. Levy AP, Levy NS, Wegner S and Goldberg MA: Transcriptional regulation of the rat vascular endothelial growth factor gene by hypoxia. *J Biol Chem* 270: 13333-13340, 1995.
12. Liu Y, Cox SR, Morita T and Kourembanas S: Hypoxia regulates vascular endothelial growth factor gene expression in endothelial cells. Identification of a 5' enhancer. *Circ Res* 77: 638-643, 1995.
13. Ebert BL, Firth JD and Ratcliffe PJ: Hypoxia and mitochondrial inhibitors regulate expression of glucose transporter-1 via distinct Cis-acting sequences. *J Biol Chem* 270: 29083-29089, 1995.
14. Firth JD, Ebert BL, Pugh CW and Ratcliffe PJ: Oxygen-regulated control elements in the phosphoglycerate kinase 1 and lactate dehydrogenase A genes: Similarities with the erythropoietin 3' enhancer. *Proc Natl Acad Sci USA* 91: 6496-6500, 1994.
15. Semenza GL, Roth PH, Fang HM and Wang GL: Transcriptional regulation of genes encoding glycolytic enzymes by hypoxia-inducible factor 1. *J Biol Chem* 269: 23757-23763, 1994.
16. Firth JD, Ebert BL and Ratcliffe PJ: Hypoxic regulation of lactate dehydrogenase A. Interaction between hypoxia-inducible factor 1 and cAMP response elements. *J Biol Chem* 270: 21021-21027, 1995.
17. Marti HJ, Bernaudin M, Bellail A, Schoch H, Euler M, Petit E and Risau W: Hypoxia-induced vascular endothelial growth factor expression precedes neovascularization after cerebral ischemia. *Am J Pathol* 156: 965-976, 2000.
18. Jin KL, Mao XO, Nagayama T, Goldsmith PC and Greenberg DA: Induction of vascular endothelial growth factor and hypoxia-inducible factor-1alpha by global ischemia in rat brain. *Neuroscience* 99: 577-585, 2000.
19. Talks KL, Turley H, Gatter KC, Maxwell PH, Pugh CW, Ratcliffe PJ and Harris AL: The expression and distribution of the hypoxia-inducible factors HIF-1alpha and HIF-2alpha in normal human tissues, cancers and tumor-associated macrophages. *Am J Pathol* 157: 411-421, 2000.

20. Semenza GL: HIF-1: Upstream and downstream of cancer metabolism. *Curr Opin Genet Dev* 20: 51-56, 2010.
21. McCluggage WG, Staats PN, Kiyokawa T and Young RH: Sex cord-stromal tumours - pure stromal tumours. In: WHO Classification of Tumours of Female Reproductive Organs. 4th edition. Kurman RJ, Carcangiu MS, Herrington CS and Young RH (Eds). International Agency for Research of Cancer. Lyon, 2014.
22. Kanai Y, Segawa H, Miyamoto Ki, Uchino H, Takeda E and Endou H: Expression cloning and characterization of a transporter for large neutral amino acids activated by the heavy chain of 4F2 antigen (CD98). *J Biol Chem* 273: 23629-23632, 1998.
23. Lee MS, Cho HC, Lee YH and Hong SR: Ovarian sclerosing stromal tumors: Gray scale and color Doppler sonographic findings. *J Ultrasound Med* 20: 413-417, 2001.